LANGMUIR

pubs.acs.org/Langmuir Article

A Robust and Efficient Method to Purify DNA-Scaffolded Nanostructures by Gravity-Driven Size Exclusion Chromatography

Alireza Ebrahimimojarad, Zhicheng Wang, Qiaochu Zhang, Akshay Shah, Jacob S. Brenner, and Jinglin Fu*

Cite This: *Langmuir* 2024, 40, 8365−8372 Read Online

ACCESS | Metrics & More | Article Recommendations | Supporting Information

ABSTRACT: In recent decades, nucleic acid self-assemblies have emerged as popular nanomaterials due to their programmable and robust assembly, prescribed geometry, and versatile functionality. However, it remains a challenge to purify large quantities of DNA nanostructures or DNA-templated nanocomplexes for various applications. Commonly used purification methods are either limited by a small scale or incompatible with functionalized structures. To address this unmet need, we present a robust and scalable method of purifying DNA nanostructures by Sepharose resin-based size exclusion. The resin column can be manually packed in-house with reusability. The separation is driven by a low-pressure gravity flow in which large DNA nanostructures are eluted first followed by smaller impurities of ssDNA and proteins. We demonstrated the efficiency of the method for purifying DNA origami assemblies and protein-immobilized DNA nanostructures. Compared to routine agarose gel electrophoresis that yields 1 μg or less of purified products, this method can purify ∼100−1000 μg of DNA nanostructures in less than 30 min, with the overall collection yield of 50−70% of crude preparation mixture. The purified nanocomplexes showed more precise activity in evaluating enzyme functions and antibody-triggered activation of complement protein reactions.

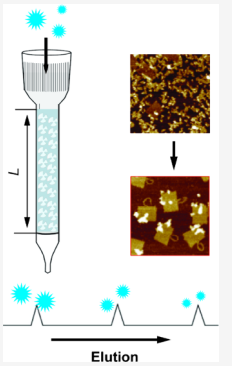

Downloaded via RUTGERS UNIV on June 3, 2024 at 14:10:10 (UTC).
See https://pubs.acs.org/sharingguidelines for options on how to legitimately share published articles.

1. INTRODUCTION

Over the past few decades, nucleic acid nanotechnology have revolutionized the field of molecular self-assembly, enabling the precise design of multidimensional nanostructures with controlled sizes and shapes.[1] DNA nanostructures, therefore, can be used as scaffolds to position functional elements on the nanoscale[2] and organize their geometric pattern.[3,4] For example, DNA nanostructures have been used to template multienzyme assemblies,[5,6] organize spatial activity of chemical reactions,[3] develop protein nanoreactors,[7] engineer biomimetic structures,[8] as well as control plasmonic nanoparticle assembly.[9] DNA nanostructures have been demonstrated to have a potential in biomedical applications, such as molecular diagnosis,[10] gene delivery,[11] vaccine development,[12] and smart delivery.[13,14] To prepare functional nanocomplexes, DNA nanostructures are often incubated with an excess of ligands, such as proteins, peptides, antigens, and nanoparticles. Therefore, it is necessary to purify functionalized nanostructures to remove excess and free ligands as well as unwanted aggregates. However, the efficient purification of DNA structures remains a challenge today; many researchers are struggling with either poor separation resolution or low yield and small scale of purification, as well as complex operation procedures consuming time and effort.

Table 1 summarizes commonly used methods to purify DNA origami and functionalized nanocomplexes as reported in the literature. Molecular weight (MW) cutoff filtration uses centrifugation to force the sample solution to pass through a size-discriminated porous membrane that only allows molecules smaller than the mass threshold to penetrate the membrane. This method is widely adopted for removing smaller and excess staple strands from large DNA assemblies. It can be easily performed for less than 1 h, with ∼50% recovery yield for regular DNA nanostructures.[15] Some publications reported the use of MW cutoff filtration to remove excess ligands and proteins by Pluronic F-127 coated filters.[12,16] However, this method is not suitable for removing large protein impurities (especially >100 kDa). MW cutoff dialysis uses a similar mechanism as MW cutoff filtration but is gentler than centrifugation and takes a longer time for dialysis exchange. Agarose gel electrophoresis (AGE) is often used to characterize the assembly of DNA nanostructures, although AGE is routinely used for a small-scale purification <1 μg with a low recovery yield (∼20−30%).[15,17] AGE is also quite laborious due to the postelectrophoresis steps of gel cut, extraction, concentration, and sometimes reassembly, as well as contamination of intercalating dyes.[7,15,18] Lin et al. reported a method of purifying DNA origami nanostructures by rate-zonal centrifugation in glycerol gradient, with a recovery yield of 40−80% at 1−100 μg.[17,19] Under high centrifugal force (300,000*g*) in density gradient media, mixed structure species were

Received: December 6, 2023
Revised: March 14, 2024
Accepted: March 29, 2024
Published: April 11, 2024

ACS Publications © 2024 American Chemical Society

https://doi.org/10.1021/acs.langmuir.3c03778
Langmuir 2024, 40, 8365−8372

Table 1. Summary of Commonly Used Methods to Purify DNA Nanostructures

purification	DNA origami	protein-modified origami	yield	scale	time consumed (h)	operation	reusable (Y/N)
MW cutoff filtration[15,16]	√	√[c]	∼50%	10−1000 μg	0.5−1[a]	simple	N
MW cutoff dialysis[12,16]	√	√[c]	>50%	10−1000 μg	6−24[a]	simple	N
agarose gel electrophoresis[15]	√	√	20−30%	0.1−1 μg	4−6	complicated	N
glycerol rate-zonal centrifugation[17,20]	√	√	40−80%	0.1−100 μg	3−6	complicated	N
PEG precipitation[21]	√		84−93%	3−4 mg	∼20[b]	simple	N
FPLC/HPLC[15,23]	√[d]	√[d]	20−40%	10−1000 μg	∼2−5	complicated	Y
gravity flow	√	√	50−70%	∼10−1000 μg	∼0.4−1	simple	Y

[a]It is estimated for three washes or buffer exchange. [b]Each centrifugation cycle lasts ∼0.5 h, whereas the dissolution of the pellet takes around 20 h. [c]For purifying protein-modified DNA origami, it may be needed to coat the filter with 5% Pluroinc F-127; only applied to small proteins (<100 kDa). [d]DNA nanostructures could be destroyed by the high-flow pressure.

separated by locating them at different gradients of the glycerol layer. This method was also applied to purify protein-modified DNA nanostructures.[20] But the glycerol gradient needs to be prepared in advance, and it requires an expensive, ultrahigh-speed centrifugation (∼300 krcf) to receive a good resolution of separation. The Dietz group reported a method using PEG precipitation to purify dense DNA nanoobjects at the milligram level with a very high recovery yield,[21] which was considered as a scale-up approach to purifiy functional DNA origami nanostructures.[22] Liquid chromatography is a standard laboratory technique used to separate a mixture by passing a fluid solvent (mobile phase) through a column filled with a solid absorbent material (stationary phase). Fast protein liquid chromatography (FPLC) and high-performance liquid chromatography (HPLC) have been used for purifying oligonucleotides, protein-oligo conjugates, and DNA nanostructures by ion exchange and size-exclusion columns.[15,23] But HPLC/FPLC is a relatively complex instrument to operate, requiring a well-trained user to run experiments. Additionally, the flow pressure of the mobile phase can also be destructive to molecular assemblies, potentially damaging assembled nanostructures.[15,24] Many agarose or porous polymer-based resins (e.g., Sepharose, mono Q) can only be used at low flow-pressure conditions (<40 bar). Thereby, the gravity flow column is often preferred as a simple and gentle separation method for soft bioparticles, such as liposomes and extracellular vesicles.[25,26] Additionally, the commonly used centrifuge-driven separation of nucleic acids includes Sephacryl or Sephadex spin columns. Compared with the gravity-driven flow column, these spin columns have a relatively poor resolution of separation. For example, it is hard to separate multiple components of different sizes as well as analyze the component distribution in the mixture. Another concern of centrifuge-driven separation is the potential vulnerability of soft nanostructures to centrifugal force, which may lead to structural damage.

Here, we present a straightforward and efficient approach of purifying DNA nanostructures and DNA-templated nanocomplexes by low-pressure, size-exclusion chromatography. The size-exclusion column can be manually prepared by packing Sepharose resins, and the separation is driven by a low-pressure gravity flow without the need for complex instrumentation. This method can purify ∼100−1000 μg of DNA nanostructures in less than 30 min, with the overall collection yield of 50−70% of crude mixture.

2. MATERIALS AND METHODS

2.1. Materials and Buffer. Pyruvate kinase (PK, type II from rabbit muscle), hexokinase (HEK, from *Saccharomyces cerevisiae*), glucose-6-phosphate dehydrogenase (G6pDH), glucose oxidase (GOX), horseradish peroxidase (HRP), phosphoenol-pyruvate (PEP), glucose, glucose 6-phosphate (G6p), β-Nicotinamide adenine dinucleotide (NAD), and adenosine 5′-diphosphate (ADP) were purchased from Sigma. NHS-DBCO was purchased from Lumiprobe. Single-stranded M13mp18 DNA (7249 nt) was bought from Bayou Biolabs. Oligonucleotides and azide or amine modified oligonucleotides were purchased from IDT. TBS (10× Tris-buffered saline) and sodium HEPES were ordered from Sigma. Sepharose CL-4B (exclusion limit >2 × 10^7 Dalton) was purchased from Cytiva. The Econo-Pac disposable chromatography 20 mL column was ordered from Bio-Rad.

TAE (1×)-12.5 mM Mg^{2+} (pH 8.0) contained 40 mM Tris, 20 mM acetic acid, 2 mM EDTA, and 12.5 mM magnesium acetate. TBS (1×)-4 mM Mg^{2+} (pH 7.5) was prepared from 10× TBS and $MgCl_2$ with pH adjusted to 7.5. Buffer preparation followed the previously published protocols.[15] All buffer solutions were prepared in deionized water and were filtered by a 0.2 μm filter.

2.2. Sepharose Column Preparation and Use. Before packing the column, it is important to shake the Sepharose resin slurry well to ensure that it is thoroughly mixed. Microliter pipettes or transfer pipettes were used to add slurry into the packing column (Econo-Pac disposable chromatography 20 mL column) 1 mL by 1 mL slowly, avoiding any trapped bubbles. The resin slurry was loaded from the side of the column. After loading the desired volume of slurry, the column was kept stationary for around 20 min to allow resins to be packed tightly. A filter cap (30 μm porous) was placed on top of the packed resin to maintain the moisture. An example of the packed column is shown in Figure S1 of the Supporting Information. The resin was washed by adding a 3× resin-bed volume of distilled water to remove any chemical contaminations. Before separation, the packed column was equilibrated with 3× column-bed volume of the buffer solution (e.g., 1× TAE-Mg^{2+}). A total of 100−200 μL of DNA nanostructures was loaded on the top of the column, and the elution was performed by adding 500 μL of the buffer each time to collect a fraction. For general separation, it may collect 10−20 mL of the eluted solution (∼20−40 fractions). After collection, the resin column was cleaned up by washing it with a 4× resin-bed volume of distilled water and was then filled in with a 1× resin-bed volume of 20% ethanol. The packed column was sealed with both top and bottom caps to main the moisture and was stored in 20% ethanol at 4 °C. The collection yield of purified DNA origami was calculated by dividing the amount of collected DNA origami by the quantity of M13 ssDNA used for the preparation.

2.3. Preparation of DNA Origami. DNA origami tiles were prepared in 1× TAE-12.5 mM Mg^{2+} buffer using published protocols.[15] Briefly, 20 nM single-stranded M13mp18 DNA (7249 nucleotides) was mixed with a 5-fold molar excess of staple stands and a 10-fold molar excess of antianchor strands. The mixture was annealed from 95 to 4 °C with the temperature gradient listed in

https://doi.org/10.1021/acs.langmuir.3c03778
Langmuir 2024, 40, 8365−8372

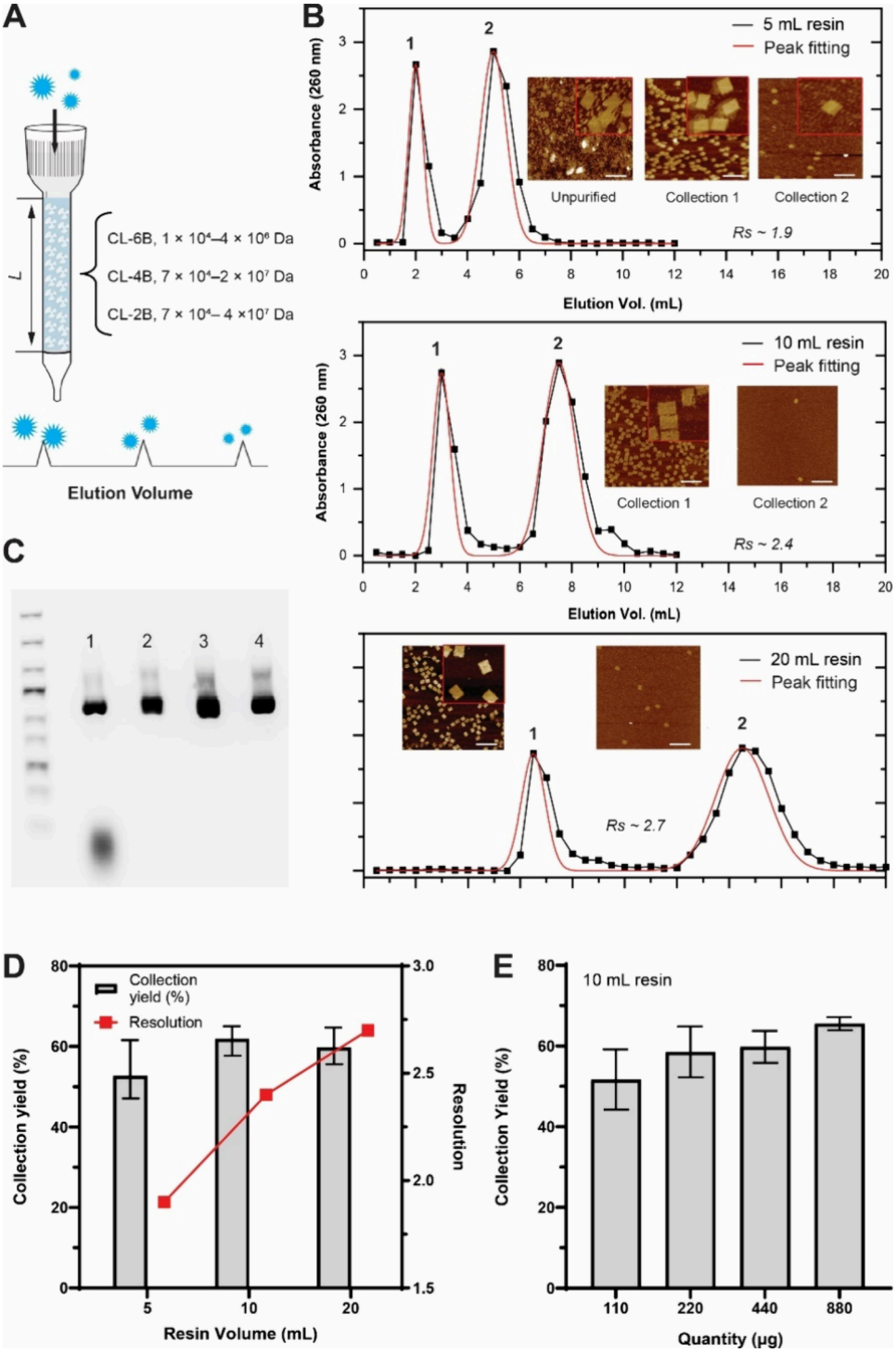

Figure 1. Sepharose resin-packed columns for the size-exclusion purification of DNA origami. (A) The conceptual illustration of the Sepharose resin-based size exclusion chromatography. (B) The size-exclusion separation of DNA origami was evaluated by different resin-bed volumes of 5, 10, and 20 mL, and the resolution of the separation (R_s) was analyzed. Insets are AFM images of collected fractions; scale bar: 400 nm. (C) Agarose gel electrophoresis to characterize the sample purification by 1100 kDa molecular weight cutoff filtration; 2, 5 mL packed column; 3, 10 mL packed column; 4, 20 mL packed column. Ladder size: 100−5000 bp. (D) Collection yield and resolution of separation for DNA origami by using 5, 10, and 20 mL packed columns. (E) Collection yield for DNA origami that was loaded for 110, 220, 220, and 880 μg by using a 10 mL packed column. Error bar: range of three replicates.

Tables S1 and S2. For a routine MW cutoff centrifugation, excess staple strands were removed by washing the solution in 1× TAE Mg^{2+} buffer (pH 8.0) with 100 kDa cutoff Amicon filters (500 μL) three times. For size exclusion purification, the assembly mixtures were directly loaded onto the Sepharose resin-packed column without the need of MW cutoff centrifugation. The concentration of DNA origami was quantified by absorbance at 260 nm, assuming an extinction coefficient of ~109,119,009 M^{-1} cm^{-1}. The detailed design of DNA origami structures is shown in Figures S2 and S3 and Tables S3−S5.

2.4. Assembly of Enzymes and Antibodies on DNA Origami Tiles. An azide-modified anchor strand (e.g., 5′ Azide-TTT CAC ACA CAC ACA CAC ACA) was purchased from IDT. The anchor

https://doi.org/10.1021/acs.langmuir.3c03778
Langmuir 2024, 40, 8365−8372

strand was hybridized to the antianchor handle on the surface of the DNA origami at a molar ratio of 1.5 (Figure S2). Enzymes or antibodies were labeled with NHS-DBCO using a similar chemistry as previously published.[16,24,27] Briefly, a 40 μL, 50 μM protein solution was added with 10× excess NHS-DBCO (20 mM stock in DMSO) into a final volume of 100 μL, 100 mM HEPES buffer (pH 8.5). The mixture was incubated on a rocker (50 rpm) for 1 h at room temperature in the dark. Excess free DBCO was then removed from the protein solution by centrifugation wash with an Amicon 30 kDa filter at 4 °C and 10,000 rpm three times. Purified DBCO-labeled protein solution was quantified by UV absorbance at 280 nm (for protein) and 309 nm (for DBCO, extinction coefficient ∼12,000 M^{-1} cm^{-1}). Azide-modified DNA origami was incubated with 10−20× DBCO-labeled enzyme or antibody solution on a rocker (50 rpm) overnight (∼12 h) at 4 °C in the dark. Then, the sample solution was ready for Sepharose resin-based size exclusion separation.

2.5. Agarose Gel Electrophoresis. Agarose gel electrophoresis was employed to analyze DNA origami purity as previously published.[15] A 1% agarose gel was prepared by dissolving 1.2 g agarose powder in 120 mL 1× TAE buffer with 12.5 mM Mg^{2+} followed by microwave heating to dissolve it. Then, 40 μL of SYBR Green (SYBR Green I Nucleic Acid Gel Stain, 10,000× concentrate) was added into the hot agarose solution followed by cooling it to form a solid gel matrix. For experiments, 20 μL of DNA sample mixed with tracking dyes was added into the loading well. Electrophoresis was carried out at a constant 200 mA in 1× TAE buffer with 12.5 mM Mg^{2+} for 2 h. The gel was imaged with a UVP ChemiDoc-It^2 instrument.

2.6. Evaluation of Enzyme Activity. Pyruvate kinase (PK) activity was evaluated by a PK-HEK cascade reaction as reported previously.[24] Briefly, an enzyme assay was performed in 1× TBS with 4 mM Mg^{2+} buffer (pH 7.5) with the addition of a substrate mixture of 1000 μM glucose, PEP, NAD^+, 10 nM HEK, 10 nM G6PDH, and 200 μM ADP. The activity was evaluated by monitoring the increased absorbance at 340 nm resulting from NADH production. Reaction curves were plotted and fit by GraphPad Prism.

2.7. C3a Protein Assay. ELISA testing was used to determine C3a production for antibody origami. For in vitro measurements, 20 μL fresh serum was incubated with 50 μL antibody-modified DNA origami for 15 min. EDTA was added to inhibit further complement activation. The C3a level was measured by using sandwich ELISA kits from BD Biosciences Company.

2.8. Atomic Force Microscope (AFM) Imaging and Dynamic Light Scattering (DLS). DNA nanostructures were imaged in liquid by AFM using the published protocol.[15] The enzyme-origami solution (2 μL) was first deposited onto a freshly cleaved mica surface (Ted Pella, Redding, CA) and was left to adsorb for 2 min. Then, 80 μL of 1× TAE-12.5 mM Mg^{2+} buffer was added to the mica for scanning in liquid. Two microliters of 100 mM Ni^{2+} was also added to enhance DNA adsorption on mica. The samples were scanned by the "Scanasyst mode in liquid mode" of Multimode 8 AFM (Bruker, Billerica, MA) using the "SCANASYST-Fluid + probe". For best imaging quality, the peak force set point was kept at ∼100−150 pN.

A Zetasizer Pro (Malvern Instruments) was used for DLS experiments as reported previously.[28] All buffers used for the DLS experiment were filtered by a 0.2 μm filter. A disposal cuvette was rinsed with distilled water three times prior to use. One hundred microliters of 10 nM DNA origami solution was added into the cuvette to measure the hydrodynamic diameter by scattering light.

2.9. Resolution of the Separation. In chromatography, the resolution of the separation (R_s) characterizes the separation between two peaks with distinct retention times "t" in a chromatogram. The R_s is fitted by Origin Pro with the function of "Peak and Baseline" using the equation

$$R_s = 2\frac{t_{R2} - t_{R1}}{w_{b1} + w_{b2}}$$

where t_R is the retention time and w_b is the peak width at the baseline.

3. RESULTS AND DISCUSSION

As described in Figure 1A, Sepharose CL-4B was selected because its exclusion limit ranged from ∼7 × 10^4 to ∼2 × 10^7 Da, which was suitable to purify M13 DNA origami (∼4.8 × 10^6 Da). For evaluating the resolution of separation, resins were filled into three columns with tightly packed volumes at 5, 10, and 20 mL. The height of the packed resin is summarized in Table 2. These packed columns were tested for separating

Table 2. Separation Resolution of DNA Origami (∼170 μg) for Different Resin Volumes

resin volume (mL)	length (cm)	resolution (R_s)	collection yield (%)
5	3.2	∼1.9	52.3
10	6.4	∼2.4	61.9
20	12.8	∼2.7	59.7

DNA origami assemblies from excess staple strands. In Figure 1B, driven by the gravity flow, the 5 mL column eluted the first peak between 1 and 2 mL, and the second peak was eluted out between 2.5 and 4.5 mL. The resolution of separation (R_s) between the two peaks was ∼1.9, which was adequate for many chromatography separations.[29] AFM imaging showed that the first peak was composed of DNA origami assemblies and the second peak was mostly free staples or smaller assemblies. As the resin volume increased to 10 mL, the resolution of separation was improved to ∼2.4, with the first peak eluted out between 2.5 and 3.5 mL and the second peak eluted out between 5.5 and 9.5 mL. The resolution of separation for 20 mL resin volume was increased to ∼2.7; however, the elution of the first peak spanned between 6 and 8 mL. The purity of collected DNA samples was analyzed by agarose gel electrophoresis as shown in Figure 1C. For the commonly used molecular weight cutoff filtration,[15] after three washes, some free ssDNA staples were still observed as lower and smeared bands on the gel. In contrast, the resin-based size exclusion collected purified DNA origami with complete removal of free ssDNA. Figure 1D shows that the yield of collected DNA origami varied between 47 and 61% for 5 mL packed resins, which could be attributed to the distribution of DNA origami in the second collected peak (Figure 1B AFM image). For 10 and 20 mL packed resins, the yield of collected DNA origami was near 60% or more. Sepharose resin-packed columns also allow for purifying large quantities of DNA samples. In Figure 1E, DNA origamis were loaded from 110 to 880 μg, and the collection yields were all above 50−60%. Considering the resolution of separation and the time consumed, we chose 10 and 20 mL resin-packed columns for later studies. The Sepharose columns were also demonstrated for the reusability by running three consecutive purifications with consistent yields of 63−65% (Figure S4). It is important to note that the collection yields of DNA origamis were calculated by dividing the amount of purified DNA origami by the quantity of M13 DNA added in the initial crude mixture for the sample preparation. Therefore, we present the overall yield of assembled and purified DNA origami that combines the synthesis and purification processes. We also evaluated the recovery yield of the Sepharose column by flowing through purified DNA origamis, which was increased to above 70% (Figure S5). Besides rectangular origami, the purification of triangular DNA origami was also demonstrated in Figure S6. The concentrations of the collected DNA origami generally ranged from 10 to 100 nM, depending on the initial amount

https://doi.org/10.1021/acs.langmuir.3c03778
Langmuir 2024, 40, 8365−8372

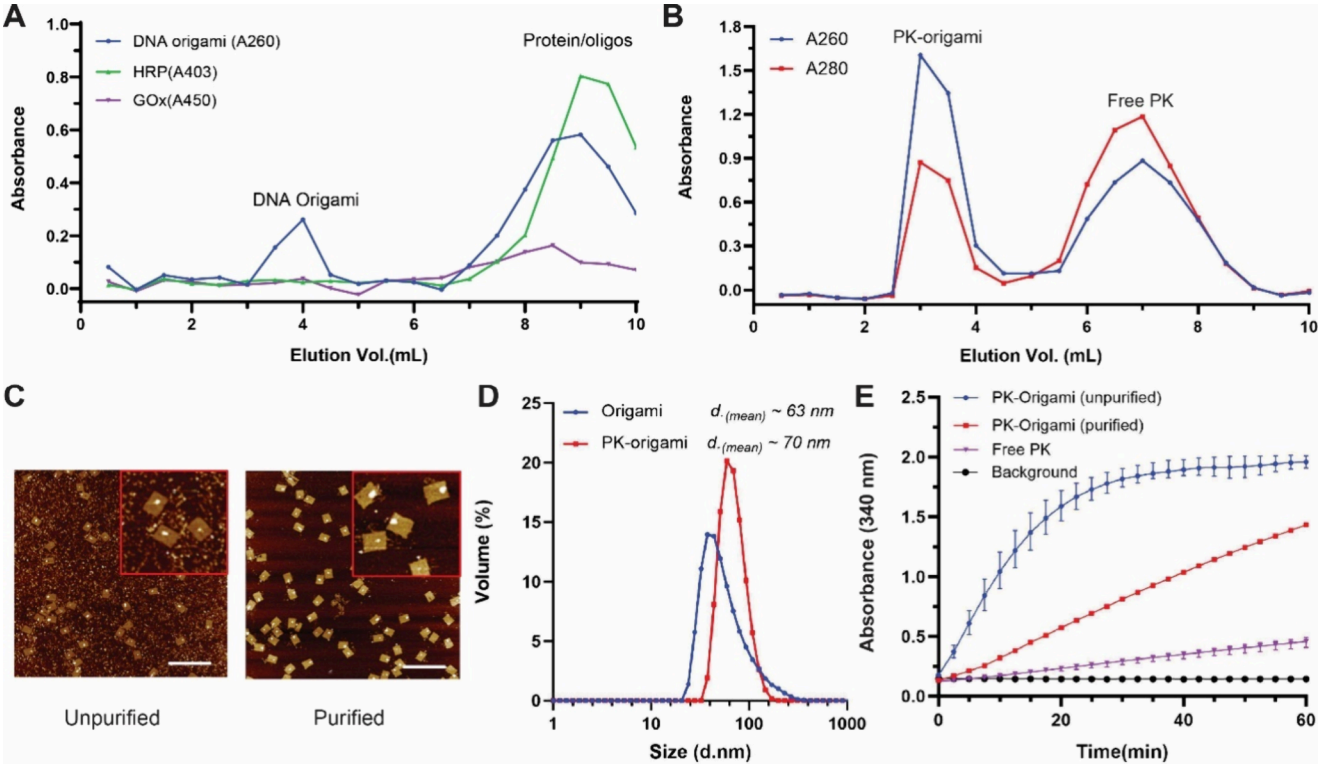

Figure 2. Purification of enzyme-modified DNA origami structures by 10 mL Sepharose resin-packed column: (A) DNA origami and free proteins (GOX, 160 kDa and HRP, 44 kDa) and (B) PK-modified DNA origami and free PK (240 kDa). (C) AFM imaging of unpurified and purified structures for PK-modified DNA origami. Scale bar: 400 nm. (D) DLS characterization of DNA origami (blue, $d._{(mean)}$ ~63 nm) and PK-modified DNA origami (red, $d._{(mean)}$ ~70 nm). (E) Enzyme activities of an unpurified mixture, purified structures, and free enzymes. Error bar, range of three replicates.

loaded for purification (Table S6). These concentration ranges are suitable for a variety of applications, including enzyme catalysis, biosensing, biophysics, and cell biology studies.

For many applications, it is necessary to functionalize DNA nanostructures with bioactive ligands such as peptides, enzymes, antibodies, and other proteins or small molecule ligands.[3−6,8] Therefore, the purification of functionalized nanostructures is crucial to remove excess free ligands and unwanted aggregates. Toward this end, we next evaluated the separation of functionalized DNA origami structures from free proteins using a Sepharose resin-packed column. In Figure 2A, DNA origami was eluted out between 3 and 4.5 mL (characterized by 260 nm absorbance), whereas color proteins of GOx (160 kDa, characterized by 450 nm absorbance) and HRP (44 kDa, characterized by 403 nm absorbance) were eluted out after 6.5 mL. This result indicated that DNA origami structures were well separated from free proteins by passing the mixture through the Sepharose column. To prepare protein-modified DNA origami, 20× excess DBCO-labeled PK (240 kDa) was added to azide-labeled DNA origami solution to ensure the high yield (~93%) of the protein assembly. In Figure 2B, the mixture was loaded to the 10 mL resin-packed column to separate PK-modified DNA origami (3−4.5 mL, A260/A280 > 1) from free, extra PK (6.5−11 mL, A260/A280 < 1). AFM imaging showed that most of the free proteins were removed from the PK origami collection (Figure 2C). The collection yield of PK origami was ~57% of the original DNA origami loaded for the purification. In Figure 2D, DLS characterized that the hydrodynamic diameter of PK origami (~70 nm) was slightly increased as compared with DNA origami (~ 63 nm). With this purification, a more precise measurement was carried out to evaluate the activity of enzyme-modified DNA nanostructures. As shown in Figure 2E, the unpurified enzyme and DNA origami mixture showed a very high activity but reached saturation in 20 min because of the presence of excess free enzymes. Purified PK origami showed a steady activity, which was ~4 times of free PK activity. This result was consistent with the previous report that DNA nanostructures could boost the activity of immobilized enzymes.[7,30] The detailed counting of PK immobilization on DNA origami is shown in Figure S7.

We also tested the purification of antibody-immobilized DNA origami by a Sepharose resin-packed column. As shown in Figure 3A, IgG-immobilized DNA origami (6−8 mL) was well separated from free IgG (12−19 mL). The collection yields of IgG origami were ~48−53% of DNA origami loaded for the preparation. AFM imaging showed the high IgG assembly yield (>90%) on the purified IgG origami for the spacing distances of 25 nm (Figure 3B) and 70 nm (Figure 3C). Detailed origami structures for antibody immobilization are described in Figure S3, and the analysis of IgG assembly yield on DNA origami is shown in Figure S8. Using click chemistry and Sepharose resin-based purification, we collected the fraction of IgG origami with the precise assembly of antibodies at designed positions for controlled spacing distances. The radiolabeled IgG elusion test showed that all origami structures carried a similar number of ~3.2 IgG/per origami (Figure S9). More AFM images of protein and IgG-modified origami were included in Figure S10. Next, we used IgG origami to study the spatial effect of the activation of

https://doi.org/10.1021/acs.langmuir.3c03778
Langmuir 2024, 40, 8365−8372

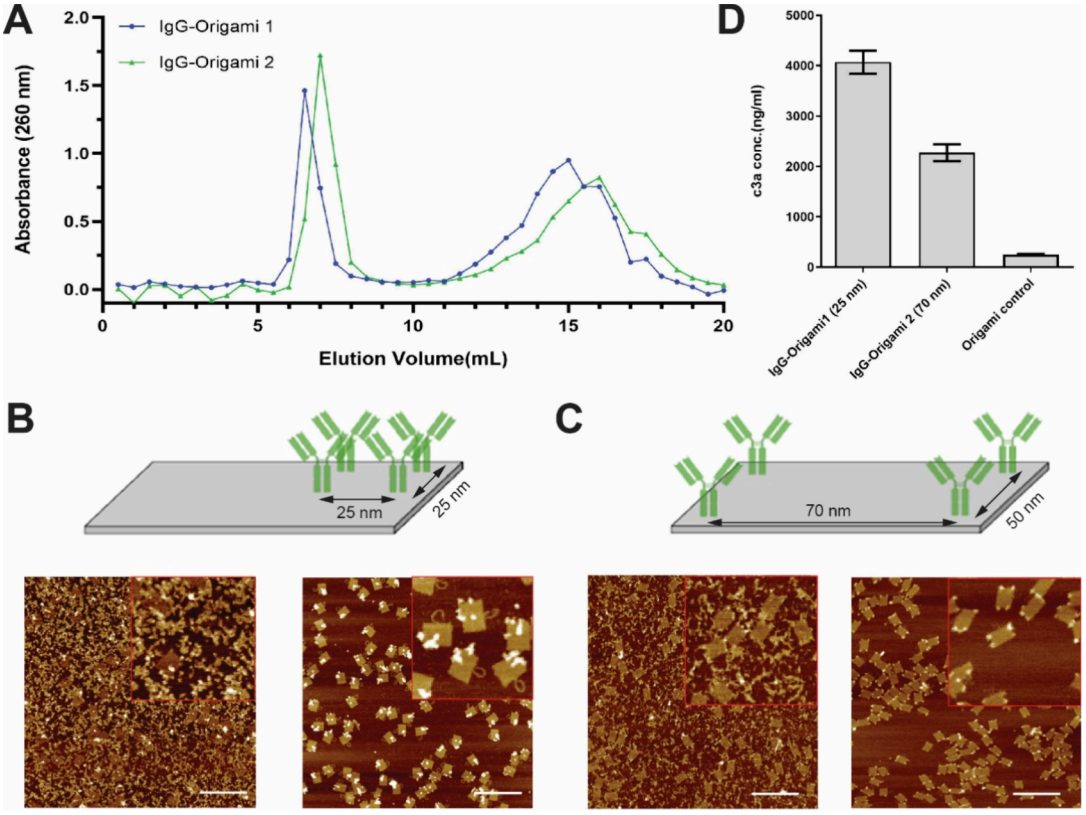

Figure 3. Purification of antibody-modified DNA origami structures. (A) Sepharose resin-packed column (20 mL) for the separation of IgG-modified DNA origami and free antibodies. IgG-Origami 1 was designed with ∼25 nm spacing distance, and IgG-Origami 2 was designed with 70 nm spacing distance. (B) AFM characterization of unpurified and purified IgG-immobilized DNA origami for the spacing distance of 25 nm and (C) 70 × 50 nm. Scale bar: 400 nm. (D) C3a production for IgG-labeled DNA origami with spacing distances of 25 and 70 nm. The control origami without immobilized IgG was also tested. Error bar, range of three replicates.

complement protein reactions,[31] which was a part of the innate immune system. C3 is the most abundant complement protein, and the activation of C3 results in the cleavage of C3 to produce C3a, which is a soluble fragment, and C3b, which forms adducts onto the surface nucleophiles (e.g., antibodies immobilized on DNA origami). C3b adducts could also catalyze more C3 cleavage at the nearby sites on the surface (called the C3 amplification loop). In Figure 3D, fresh serum was incubated with IgG-DNA origami for initiating C3a production. IgG origami with a 25 nm spacing distance triggered more C3a production than IgG origami with a 70 nm spacing distance. This result suggested that the spreading of C3 reaction and C3 "amplification loop" on the surface was affected by the spatial arrangement of surface nucleophiles, in which the short distance between nucleophile sites spread the C3 reaction more quickly on the surface of particles.

4. CONCLUSIONS

In summary, we have developed a rapid and robust method for purifying DNA nanostructures by Sepharose resin-based size-exclusion chromatography. We evaluated the separation resolution and collection yield depending on the resin-packed volume and sample loading quantity. The method has the advantages of (1) simple in-house preparation and operation driven by the gravity flow; (2) scale up to purify hundreds of μg DNA nanostructures; and (3) consistent collection yield ∼50−70%. For smaller sample scale <100 μg, it could be carried out by using less resin volume and more narrowly packed column to increase the length of gel bed. We demonstrated the usefulness of this method for purifying enzyme-immobilized DNA origami, and purified nanostructures produced more precise activities for evaluating catalytic performance. Further, we used this method to purify antibody-immobilized DNA origami with controlled spacing distances between antibodies. These precisely assembled antibody nanocomplexes were used to study the distance-dependent activation of C3 reaction on the surface of DNA origami. It could help interpret the spatial dependent mechanism of complement protein cascades for regulating immune response. It should be noted that Sepharose resin is best suited for soft nanostructures assembled by biomolecules, like nucleic acids, lipids, peptides, and proteins. For inorganic solid nanoparticles such as gold nanoparticles, they tend to be trapped in resins and are difficult to elute out (Figure S11). The Sepharose resin-based size exclusion can help address the technical challenge of purifying DNA nanostructures or DNA-scaffolded nanocomplexes on a large scale. This method can contribute to the advancement of nucleic acid nanotechnology into various applications, such as biocatalysis, smart materials, biosensing, and therapeutics.

■ ASSOCIATED CONTENT

Supporting Information

The Supporting Information is available free of charge at https://pubs.acs.org/doi/10.1021/acs.langmuir.3c03778.

Example of packed column (Figure S1); DNA origami maps (Figures S2 and S3); reusability of the column (Figure S4); recovery yield of pure DNA origami

https://doi.org/10.1021/acs.langmuir.3c03778
Langmuir 2024, 40, 8365−8372

(Figure S5); purification of triangular DNA origami (Figure S6); PK assembly yield on DNA origami (Figure S7); IgG assembly yield on DNA origami (Figure S8); elution analysis of radiolabeled IgG (Figure S9); AFM images of various assembled nanostructures (Figure S10); GNPs trapped within the column (Figure S11); thermal annealing program for preparing DNA nanostructures (Tables S1 and S2); DNA sequences (Table S3−S5); and concentration of the collected sample (Table S6) (PDF)

AUTHOR INFORMATION

Corresponding Author

Jinglin Fu − *Department of Chemistry and Center for Computational and Integrative Biology, Rutgers University−Camden, Camden, New Jersey 08102, United States*; orcid.org/0000-0002-0814-0089; Email: jinglin.fu@rutgers.edu

Authors

Alireza Ebrahimimojarad − *Center for Computational and Integrative Biology, Rutgers University−Camden, Camden, New Jersey 08102, United States*

Zhicheng Wang − *Department of Systems Pharmacology and Translational Therapeutics, Perelman School of Medicine, University of Pennsylvania, Philadelphia, Pennsylvania 19104, United States*

Qiaochu Zhang − *Center for Computational and Integrative Biology, Rutgers University−Camden, Camden, New Jersey 08102, United States*

Akshay Shah − *Department of Chemistry, Rutgers University−Camden, Camden, New Jersey 08102, United States*

Jacob S. Brenner − *Department of Systems Pharmacology and Translational Therapeutics, Perelman School of Medicine, University of Pennsylvania, Philadelphia, Pennsylvania 19104, United States*

Complete contact information is available at: https://pubs.acs.org/10.1021/acs.langmuir.3c03778

Author Contributions

A.E., Z.W., and J.F. designed experiments. A.E., Z.W., Q.Z., and A.S. ran experiments and collected data. The manuscript was drafted by A.E. and J.F and was revised by all authors. All authors have given approval to the final version of the manuscript.

Notes

The authors declare no competing financial interest.

ACKNOWLEDGMENTS

This work was supported by a PECASE award to J.F. (W911NF1910240), a DoD DURIP (W911NF2010107), an NSF MRI (2215917), and an NSF PFI award (2141141). J.F. also appreciates the support from Busch Biomedical Grant. J.B. is funded by NIH grants R01-HL160694 and R01-HL153510. Z.W. is supported by a PhRMA Foundation Postdoctoral Fellowship. A.E. and Q.Z. appreciate the support from Rutgers-Camden Chancellor's Grant for Independent Student Research. A.S. appreciates the support of the Arts and Sciences OMIC Summer Research Grant and Undergraduate Apprenticeship from AEOP. The authors are grateful to the Equipment Leasing Funds from the State of New Jersey.

REFERENCES

(1) Krishnan, Y.; Seeman, N. C. Introduction: Nucleic Acid Nanotechnology. *Chem. Rev.* **2019**, *119*, 6271−6272.

(2) Bathe, M.; Rothemund, P. W. K. DNA Nanotechnology: A foundation for Programmable Nanoscale Materials. *MRS Bull.* **2017**, *42*, 882−888.

(3) Fu, J.; Liu, M.; Liu, Y.; Yan, H. Spatially-Interactive Biomolecular Networks Organized by Nucleic Acid Nanostructures. *Acc. Chem. Res.* **2012**, *45*, 1215−1226.

(4) Zhan, P.; Peil, A.; Jiang, Q.; Wang, D.; Mousavi, S.; Xiong, Q.; Shen, Q.; Shang, Y.; Ding, B.; Lin, C.; et al. Recent Advances in DNA Origami-Engineered Nanomaterials and Applications. *Chem. Rev.* **2023**, *123*, 3976−4050.

(5) Fu, J.; Wang, Z.; Liang, X. H.; Oh, S. W.; St. Iago-McRae, E.; Zhang, T. DNA-Scaffolded Proximity Assembly and Confinement of Multienzyme Reactions. *Topics Curr. Chem.* **2020**, *378*, 38.

(6) Fu, J.; Liu, M.; Liu, Y.; Woodbury, N. W.; Yan, H. Interenzyme Substrate Diffusion for an Enzyme Cascade Organized on Spatially Addressable DNA Nanostructures. *J. Am. Chem. Soc.* **2012**, *134*, 5516−5519.

(7) Zhao, Z.; Fu, J.; Dhakal, S.; Johnson-Buck, A.; Liu, M.; Zhang, T.; Woodbury, N. W.; Liu, Y.; Walter, N. G.; Yan, H. Nanocaged enzymes with enhanced catalytic activity and increased stability against protease digestion. *Nat. Commun.* **2016**, *7*, 10619.

(8) Fu, J.; Oh, S. W.; Monckton, K.; Arbuckle-Keil, G.; Ke, Y.; Zhang, T. Biomimetic Compartments Scaffolded by Nucleic Acid Nanostructures. *Small* **2019**, *15*, No. 1900256.

(9) Liu, N.; Liedl, T. DNA-Assembled Advanced Plasmonic Architectures. *Chem. Rev.* **2018**, *118*, 3032−3053.

(10) Oh, S. W.; Pereira, A.; Zhang, T.; Li, T.; Lane, A.; Fu, J. DNA-Mediated Proximity-Based Assembly Circuit for Actuation of Biochemical Reactions. *Angew. Chem., Int. Ed.* **2018**, *57*, 13086−13090.

(11) Wu, X.; Yang, C.; Wang, H.; Lu, X.; Shang, Y.; Liu, Q.; Fan, J.; Liu, J.; Ding, B. Genetically Encoded DNA Origami for Gene Therapy In Vivo. *J. Am. Chem. Soc.* **2023**, *145*, 9343−9353.

(12) Veneziano, R.; Moyer, T. J.; Stone, M. B.; Wamhoff, E.-C.; Read, B. J.; Mukherjee, S.; Shepherd, T. R.; Das, J.; Schief, W. R.; Irvine, D. J.; et al. Role of nanoscale antigen organization on B-cell activation probed using DNA origami. *Nat. Nanotechnol.* **2020**, *15*, 716−723.

(13) Zhang, T.; Nong, J.; Alzahrani, N.; Wang, Z.; Oh, S. W.; Meier, T.; Yang, D. G.; Ke, Y.; Zhong, Y.; Fu, J. Self-Assembly of DNA−Minocycline Complexes by Metal Ions with Controlled Drug Release. *ACS Appl. Mater. Interfaces* **2019**, *11*, 29512−29521.

(14) Jiang, Q.; Shang, Y.; Xie, Y.; Ding, B. DNA Origami: From Molecular Folding Art to Drug Delivery Technology. *Adv. Mater.* **2023**, No. 2301035.

(15) Fu, J.; Yang, Y. R.; Dhakal, S.; Zhao, Z.; Liu, M.; Zhang, T.; Walter, N. G.; Yan, H. Assembly of multienzyme complexes on DNA nanostructures. *Nat. Protoc.* **2016**, *11*, 2243−2273.

(16) Knappe, G. A.; Wamhoff, E.-C.; Read, B. J.; Irvine, D. J.; Bathe, M. In Situ Covalent Functionalization of DNA Origami Virus-like Particles. *ACS Nano* **2021**, *15*, 14316−14322.

(17) Lin, C.; Perrault, S. D.; Kwak, M.; Graf, F.; Shih, W. M. Purification of DNA-origami nanostructures by rate-zonal centrifugation. *Nucleic Acids Res.* **2013**, *41*, e40−e40.

(18) Bellot, G.; McClintock, M. A.; Lin, C.; Shih, W. M. Recovery of intact DNA nanostructures after agarose gel-based separation. *Nat. Methods* **2011**, *8*, 192−194.

(19) Yang, Y.; Wang, J.; Shigematsu, H.; Xu, W.; Shih, W. M.; Rothman, J. E.; Lin, C. Self-assembly of size-controlled liposomes on DNA nanotemplates. *Nat. Chem.* **2016**, *8*, 476−483.

(20) Fisher, P. E.; Shen, Q.; Akpinar, B.; Davis, L. K.; Chung, K. K. H.; Baddeley, D.; Šarić, A.; Melia, T. J.; Hoogenboom, B. W.; Lin, C.; Lusk, C. P. A Programmable DNA Origami Platform for Organizing Intrinsically Disordered Nucleoporins within Nanopore Confinement. *ACS Nano* **2018**, *12*, 1508−1518.

(21) Stahl, E.; Martin, T. G.; Praetorius, F.; Dietz, H. Facile and Scalable Preparation of Pure and Dense DNA Origami Solutions. *Angew. Chem., Int. Ed.* **2014**, *53*, 12735−12740.
(22) Shaw, A.; Benson, E.; Högberg, B. Purification of Functionalized DNA Origami Nanostructures. *ACS Nano* **2015**, *9*, 4968−4975.
(23) Fu, J.; Yang, Y. R.; Johnson-Buck, A.; Liu, M.; Liu, Y.; Walter, N. G.; Woodbury, N. W.; Yan, H. Multi-enzyme complexes on DNA scaffolds capable of substrate channelling with an artificial swinging arm. *Nat. Nanotechnol.* **2014**, *9*, 531−536.
(24) Wang, Z.; St. Iago-Mcrae, E.; Ebrahimimojarad, A.; Won Oh, S.; Fu, J. Modulation of Enzyme Cascade Activity by Local Substrate Enrichment and Exclusion on DNA Nanostructures. *Langmuir* **2022**, *38*, 12594−12601.
(25) Jung, J. H.; Back, W.; Yoon, J.; Han, H.; Kang, K. W.; Choi, B.; Jeong, H.; Park, J.; Shin, H.; Hur, W.; Choi, Y.; Hong, S.; Kim, H. K.; Park, Y.; Park, J. H.; et al. Dual size-exclusion chromatography for efficient isolation of extracellular vesicles from bone marrow derived human plasma. *Sci. Rep.* **2021**, *11*, 217.
(26) Xu, R.; Fitts, A.; Li, X.; Fernandes, J.; Pochampally, R.; Mao, J.; Liu, Y. M. Quantification of Small Extracellular Vesicles by Size Exclusion Chromatography with Fluorescence Detection. *Anal. Chem.* **2016**, *88*, 10390−10394.
(27) Hood, E. D.; Greineder, C. F.; Shuvaeva, T.; Walsh, L.; Villa, C. H.; Muzykantov, V. R. Vascular Targeting of Radiolabeled Liposomes with Bio-Orthogonally Conjugated Ligands: Single Chain Fragments Provide Higher Specificity than Antibodies. *Bioconjugate Chem.* **2018**, *29*, 3626−3637.
(28) Fu, J.; Nguyen, K. Reduction of Promiscuous Peptides-Enzyme Inhibition and Aggregation by Negatively Charged Biopolymers. *ACS Applied Bio Materials* **2022**, *5*, 1839−1845.
(29) Ornaf, R. M.; Dong, M. W. In Ahuja, S.; Dong, M. W. (eds.), *Sep. Sci. Technol.*. Academic Press 2005, Vol. *6*, pp 19−45.
(30) Collins, J.; Zhang, T.; Oh, S.; Maloney, R.; Fu, J. DNA-Crowded Enzyme Complexes with Enhanced Activities and Stabilities. *Chem. Commun.* **2017**, *53*, 13059−13062.
(31) Wang, Z.; Brenner, J. S. The Nano-War Against Complement Proteins. *AAPS J.* **2021**, *23*, 105.

https://doi.org/10.1021/acs.langmuir.3c03778
Langmuir 2024, 40, 8365−8372